

## Antiphased states in intracavity second-harmonic generation: Stability of the periodic solutions

Jing-Yi Wang\* and Paul Mandel†

*Université Libre de Bruxelles, Campus Plaine Code Postal 231, 1050 Bruxelles, Belgium*

(Received 21 February 1995)

We study the self-pulsing solutions which emerge from the steady state via a Hopf bifurcation in a laser with intracavity second-harmonic generation. Our main result is the construction of periodic solutions and the derivation of explicit amplitude equations which rule the stability of these periodic solutions. In this way, we have been able to substantiate the classification into four classes of periodic solutions with simple phase and amplitude relations. Near the Hopf bifurcation, the periodic solutions are stable and the sum over the individual mode intensities is not periodic but constant, a signature of antiphase dynamics in this system. A fifth class of periodic solutions has been found numerically where the sum over all modal intensities is periodic. Finally, a numerical analysis complements these results and shows that the phase relations which characterize antiphase dynamics are maintained throughout the route to chaos and in the first chaotic domain when the pump parameter is increased.

PACS number(s): 42.50.Ne, 42.60.Mi

### I. INTRODUCTION

Antiphase dynamics (AD) is a property displayed by systems in which  $N$  degrees of freedom oscillate with a strong phase correlation. In laser physics, this type of dynamics is now well established for the self-pulsing state of intracavity second-harmonic generation (ISHG) [1–7] and for pulsing lasers [8–12] that can be described by the Tang, Stutz, and deMars rate equations [13] with gain or loss modulation. For periodic solutions, antiphase dynamics is a highly ordered state in which the modal intensities are periodic but the total intensity is either periodic or constant. This requires a strong correlation among the phases of the modal intensities. A generalization of this property for transient, noisy, and chaotic dynamics has been observed experimentally, analytically, or numerically. A short review of these extensions and a list of references can be found in [14].

In the case of periodic states, the classic example of AD is the experimental observation made by Wiesenfeld *et al.* [1]. They showed that an ISHG laser could oscillate on three modes which self-pulse (AM modulation) in such a way that each mode is “on” successively. Numerical simulations of the relevant equations indicate that all modes have the same time dependence but they are phase shifted by a constant amount ( $\frac{1}{3}$  of the period in this case) so that the total intensity is also in a periodic state but with a frequency which is three times larger than the modal frequency. The fact that the low frequency which characterizes the modal intensity dynamics disappears from the power spectrum of the total intensity seems to be the signature of AD which is best generalized to more complex situations.

In a recent paper [5], we have analyzed the periodic

solutions occurring in the equations proposed by Roy, Bracikowski, and James [15] to describe ISHG:

$$\eta dI_m/dt = I_m \left[ G_m - \alpha + g\epsilon I_m - 2g\epsilon \sum_{r=1}^M I_r - 2g_1\epsilon \sum_{r=1}^P J_r \right], \quad (1)$$

$$\eta dJ_p/dt = J_p \left[ H_p - \alpha + g\epsilon J_p - 2g\epsilon \sum_{r=1}^P J_r - 2g_1\epsilon \sum_{r=1}^M I_r \right], \quad (2)$$

$$dG_m/dt = \gamma - G_m \left[ 1 + (1-\beta)I_m + \beta \sum_{r=1}^M I_r + \beta \sum_{r=1}^P J_r \right], \quad (3)$$

$$dH_p/dt = \gamma - H_p \left[ 1 + (1-\beta)J_p + \beta \sum_{r=1}^P J_r + \beta \sum_{r=1}^M I_r \right], \quad (4)$$

with  $\eta = \tau_c / \tau_f$  where  $\tau_c$  and  $\tau_f$  are the cavity round-trip time and fluorescence lifetime, respectively.  $\alpha$  is the cavity loss parameter,  $\gamma$  is the small signal gain which is related to the pump rate,  $\beta$  is the cross-saturation parameter, and  $g$  is a geometrical factor whose value depends on the phase delays of the amplifying and doubling crystals and on the angle between the fast axes of these two crystals. We have assumed that  $\alpha$ ,  $\beta$ , and  $\gamma$  are mode independent, in good agreement with the experimental results [1]. The electric field modes can oscillate in one of two orthogonal polarizations. There are  $M$  modes in one field polarization ( $m = 1, 2, \dots, M$ ) and  $P$  modes in the orthogonal polarization ( $p = 1, 2, \dots, P$ ) with  $M + P = N$ .  $I_m$  and  $G_m$  or  $J_p$  and  $H_p$  are, respectively, the intensity and the nonlinear gain associated with the  $m$ th or  $p$ th longitudinal mode. The mode-mode coupling constant is  $g$  when the two modes have the same polarization and

\*Electronic address: JWANG@ULB.AC.BE

†Electronic address: PMANDEL@ULB.AC.BE

$g_1 = 1 - g$  when the two modes have orthogonal polarizations.  $\epsilon$  is a nonlinear coefficient whose value depends on the properties of the potassium trihydrogen phosphate (KTP) crystal; it is a measure of the conversion efficiency of the intensity at the fundamental frequency into the frequency-doubled intensity.

An asymptotic analysis of Eqs. (1)–(4) has to be based on the orders of magnitudes suggested by experiments for the various parameters:

$$\epsilon \ll 1, \quad \eta \ll 1, \quad \alpha, \beta, \gamma, g, \epsilon/\eta = O(1), \quad (5)$$

with the physical restrictions  $0 < g < 1$  and  $0 < \beta < 1$ . In [5], we made an expansion of the amplitude of the periodic solutions of Eqs. (1)–(4) in powers of  $\epsilon^{1/4}$ . The motivation for this unusual scaling was to avoid an expansion in terms of a small parameter  $0 < \delta \ll 1$  defined through  $f = f_h \pm \delta^2$ , where  $f$  is a control parameter such as  $\alpha$ ,  $\beta$ , or  $\gamma$  and  $f_h$  is the value of  $f$  at the Hopf bifurcation. The  $\epsilon^{1/4}$  expansion was only partially successful since it produced a set of degenerate amplitude equations for the oscillating solutions. From these equations, the stability of the solutions could not be assessed at least to dominant order in the small parameter. However, a positive result of that analysis was the occurrence of sum rules which enabled a classification of the periodic solutions.

In this paper, we propose a more traditional analysis in the vicinity of the bifurcation point. This analysis leads to a definite answer on the stability problem and the structure of the bifurcation equations explains the difficulties met in the previous analysis. The technical problem is that the amplitudes are functions of at least two small parameters, namely,  $\epsilon$  and  $\eta$ , and of the expansion parameter if it is distinct from  $\epsilon$  and  $\eta$ . The limit

$$I_{h1} = I_{h10} = \frac{1}{g\epsilon/\eta - [1 + (N-1)\beta]}, \quad (9)$$

$$I_{h2} = I_{h20} + O(\eta),$$

$$I_{h20} = \frac{1}{\{4MP/N - [(8MP - N)/N]g\}\epsilon/\eta - [1 + (N-1)\beta]}. \quad (10)$$

Note that if all modes oscillate with the same polarization the destabilization occurs at  $I_{h1}$  while if  $M = P = 1$  the destabilization occurs at  $I_{h2}$  for all  $g$ . A third Hopf bifurcation has also been found but it requires the non-physical value  $g > 1$ . Therefore we shall not analyze it here.

## II. BIFURCATION ANALYSIS

At the Hopf bifurcation, periodic solutions emerge with a frequency given by a purely imaginary root of the characteristic polynomial. The two frequencies are

$$\omega_1^2 = I_{h1} G_{h1} (1 - \beta) / \eta - g \epsilon I_{h1} \gamma_{h1} / (\eta G_{h1}), \quad (11)$$

$$\omega_2^2 = I_{h2} G_{h2} (1 - \beta) / \eta + O(1), \quad (12)$$

where  $\gamma_{hj}$  is the solution of the implicit equation

where all three parameters tend to zero is singular and the relative magnitude between these small parameters defines different limits.

Our starting point will be the steady-state solution in which all modes with the same polarization have the same intensity and nonlinear gain:  $I_m = I_s$ ,  $G_m = G_s$ ,  $m = 1, 2, \dots, M$ , and  $J_p = J_s$ ,  $H_p = H_s$ ,  $p = 1, 2, \dots, P$ . This steady state is not the only possible steady solution of (1)–(4). However, for the parameter values realized in [1], i.e.,  $\epsilon \sim 10^{-5}$ , it is the stable state with the lowest linear gain or pump parameter  $\gamma$ . As shown in [4] and [5], this steady state is stable if and only if (iff)

$$g < \frac{\eta}{\epsilon} \frac{\gamma}{I_s G_s} = \frac{\eta}{\epsilon} \gamma \frac{1 + (N-1)\beta}{\gamma - \alpha} + O(\eta), \quad (6)$$

$$g > \frac{1}{8MP - N} \left[ 4MP - N \gamma \frac{\eta}{\epsilon} \frac{1 + (N-1)\beta}{\gamma - \alpha} \right] + O(\eta). \quad (7)$$

If all modes oscillate in the same polarization (either  $M = 0$  or  $P = 0$ ), the only stability condition is (6). If  $M = P = 1$ , the only stability condition is (7). Otherwise, neglecting the  $O(\eta)$  correction in (6) and (7), these two inequalities are compatible only if the following relation holds:

$$\frac{\eta}{\epsilon} \gamma \frac{1 + (N-1)\beta}{\gamma - \alpha} > \frac{1}{2}, \quad (8)$$

which provides a necessary condition of stability for the steady-state solution. If the condition (8) is not satisfied, the steady solution will be destabilized via a Hopf bifurcation to a time-periodic solution for  $\beta < 1$  and  $\epsilon \ll 1$ . In general, the Hopf bifurcation occurs at  $I_{h1}$  for  $g > \frac{1}{2}$  and at  $I_{h2}$  for  $g < \frac{1}{2}$ :

$I_{hj}(\gamma) = I_s(\gamma)$  for  $j = 1$  or  $2$ . In the vicinity of the Hopf bifurcation, we seek solutions of Eqs. (1)–(4) of the form

$$\begin{aligned} I_m &= I_h + x_m(\delta, T, \sigma), & J_p &= J_h + y_p(\delta, T, \sigma), \\ G_m &= G_h + u_m(\delta, T, \sigma), & H_p &= H_h + v_p(\delta, T, \sigma), \end{aligned} \quad (13)$$

where  $x_m$ ,  $y_p$ ,  $u_m$ , and  $v_p$  can be expanded in powers of  $\delta$  as follows:

$$z(\delta, t) = \delta z_1(T, \sigma) + \delta^2 z_2(T, \sigma) + \delta^3 z_3(T, \sigma) + O(\delta^4), \quad (14)$$

and the functions  $I_h$ ,  $J_h$ ,  $G_h$ , and  $H_h$  refer to the intensities and nonlinear gains at either of the two Hopf bifurcations. The small parameter  $\delta$ , the fast time  $T$ , and the slow time  $\sigma$  are defined by

$$\begin{aligned} \gamma &= \gamma_h + a_2 \delta^2, \quad 0 < \delta \ll 1, \quad a_2 = \pm 1, \\ T &= \omega t, \quad \sigma = \delta^2 t, \end{aligned} \tag{15}$$

where  $\omega = \omega_1$  if  $I_h = I_{h1}$  and  $\omega = \omega_2$  if  $I_h = I_{h2}$ . Thus we seek  $2N$  amplitudes  $x_m, u_m, y_p,$  and  $v_p$  which are  $2\pi$ -periodic functions of  $T$  in the long-time limit  $T \rightarrow \infty$ . The strategy we follow in this paper is to seek the periodic solutions for  $0 < \delta \ll 1$  with  $\epsilon = O(1)$  and  $\eta = O(1)$ . In other terms,  $\delta$  is the small parameter whereas  $\epsilon$  and  $\eta$  are fixed constant parameters. This will lead to equations whose coefficients are usually too complex to be analyzed and we shall then expand these coefficients in powers of  $\epsilon$  and  $\eta$ . This procedure amounts to studying the limit

$$\delta \rightarrow 0, \quad \epsilon \rightarrow 0, \quad \eta \rightarrow 0, \quad \delta/\epsilon \rightarrow 0, \quad \epsilon/\eta = O(1). \tag{16}$$

This last expansion will be made explicitly in the bifurcation equations (48), (51), and (52). It will appear then that only minimal qualitative information is needed from the limit (16) to proceed with the analysis.

### A. The first-order problem

The first-order amplitudes  $x_{m1}, y_{p1}, u_{m1},$  and  $v_{p1}$  satisfy the evolution equations

$$\omega \eta \frac{\partial x_{m1}}{\partial T} = \left[ u_{m1} + g \epsilon x_{m1} - 2g \epsilon \sum_{r=1}^M x_{r1} - 2g_1 \epsilon \sum_{r=1}^P y_{r1} \right] I_h, \tag{17}$$

$$\omega \eta \frac{\partial y_{p1}}{\partial T} = \left[ v_{p1} + g \epsilon y_{p1} - 2g \epsilon \sum_{r=1}^P y_{r1} - 2g_1 \epsilon \sum_{r=1}^M x_{r1} \right] J_h, \tag{18}$$

$$\begin{aligned} \omega \frac{\partial u_{m1}}{\partial T} &= -G_h \left[ (1-\beta)x_{m1} + \beta \sum_{r=1}^M x_{r1} + \beta \sum_{r=1}^P y_{r1} \right] \\ &\quad - \frac{\gamma_h}{G_h} u_{m1}, \end{aligned} \tag{19}$$

---


$$\begin{aligned} \varphi_j &= \text{col}[S(\delta_j, M-1), -1, \mathcal{L}_1 S(\delta_j, M-1), -\mathcal{L}_1], \quad j=1, 2, \dots, M-1, \\ \mathcal{L}_1 &= i\omega \eta / I_{h1} - g \epsilon = (\beta - 1)G_{h1} / (i\omega + \gamma_{h1} / G_{h1}), \end{aligned} \tag{24}$$

where  $S(\delta_j, N) = \delta_{1j}, \delta_{2j}, \dots, \delta_{Nj}$  is a sequence of Kronecker symbols. These eigenvectors are associated with antiphased solutions in which only a pair of modes is excited but with opposite phases.

With these eigenvectors we construct the general periodic solution of Eqs. (17) and (19):

$$x_{m1} = \alpha_m(\sigma) e^{iT} + \text{c.c.}, \quad u_{m1} = \mathcal{L}_1 \alpha_m(\sigma) e^{iT} + \text{c.c.}, \tag{25}$$

where the coefficients satisfy the sum rule

$$\sum_{m=1}^M \alpha_m(\sigma) = 0. \tag{26}$$

The functions  $\alpha_m(\sigma)$  will be determined by requiring that the solutions at order  $\delta^3$  be periodic.

$$\begin{aligned} \omega \frac{\partial v_{p1}}{\partial T} &= -H_h \left[ (1-\beta)y_{p1} + \beta \sum_{r=1}^M x_{r1} + \beta \sum_{r=1}^P y_{r1} \right] \\ &\quad - \frac{\gamma_h}{H_h} v_{p1}. \end{aligned} \tag{20}$$

This problem can be formulated as the  $2N \times 2N$  matrix equation  $\partial z / \partial T = \mathcal{M}z$  where  $z$  is the column vector

$$z = \text{col}[S(x_1, M), S(y_1, P), S(u_1, M), S(v_1, P)]$$

and  $\mathcal{M}$  is a  $2N \times 2N$  constant matrix. The notation adopted throughout this paper is that  $S(x_1, N)$  with  $N$  integer is the sequence  $x_{11}, x_{21}, \dots, x_{N1}$ . Seeking periodic solutions of the form  $z(T) \sim \exp i\lambda T$  leads to a characteristic equation which we discuss in the relevant cases.

### 1. $M = N, P = 0$

The bifurcation takes place at  $I_h = I_{h1}$ . The characteristic equation is

$$(a - b)^{M-1} [a + (M-1)b] = 0, \tag{21}$$

where

$$\begin{aligned} a &= \left[ \frac{i\omega \eta}{I_{h1}} \lambda + g \epsilon \right] \left[ i\omega \lambda + \frac{\gamma_{h1}}{G_{h1}} \right] + G_{h1}, \\ b &= 2g \epsilon \left[ i\omega \lambda + \frac{\gamma_{h1}}{G_{h1}} \right] + \beta G_{h1}. \end{aligned} \tag{22}$$

The solutions of Eq. (21) are

$$\lambda_1^2 = 1, \quad \lambda_2 = \frac{iM}{\omega} \frac{\gamma_{h1}}{G_{h1}} \pm \left[ \frac{1 + (M-1)\beta}{1-\beta} \right]^{1/2} + O(\eta). \tag{23}$$

The solutions associated with the eigenvalue  $\lambda_2$  vanish for  $T \rightarrow \infty$ . The eigenvalue  $\lambda_1^2$  is degenerate and has  $M-1$  eigenvectors which can be written as

### 2. $M$ and $P \geq 1$

The characteristic equation is

$$(a - b)^{N-2} \{ [a + (M-1)b][a + (P-1)b] - MPc^2 \} = 0, \tag{27}$$

$$c = (i\omega \lambda + \gamma_h / G_h) 2g_1 \epsilon + \beta G_h,$$

and the definition (22) for  $a$  and  $b$ . Using the relations (5) we neglected the difference between  $I_h$  and  $J_h$  and between  $G_h$  and  $H_h$ . The discussion will be different depending on which of the two Hopf bifurcations occurs first.

(a)  $I_h = I_{h1}$ . The solutions of Eq. (27) are

$$\lambda_1^2 = 1, \quad \lambda_2 = \pm 1 + \frac{i}{\omega} \frac{2MP}{N} \frac{\gamma_{h1}}{G_{h1}} \left[ 1 - \frac{g_1}{g} \right] + O(\eta),$$

$$\lambda_3 = \pm \left[ \frac{1 + (N-1)\beta}{1-\beta} \right]^{1/2} + \frac{2i}{\omega} \frac{\gamma_{h1}}{G_{h1}} \left[ M^2 + P^2 + MP \frac{g_1}{g} \right] + O(\eta).$$

The third root does not contribute to the long-time limit since  $\text{Re}(i\lambda_3) < 0$ . The real part of  $i\lambda_2$  is positive for  $g < \frac{1}{2}$  and negative for  $g > \frac{1}{2}$ . Thus we only consider the domain  $g > \frac{1}{2}$ . The eigenvalue  $\lambda_1$  is degenerate and has  $N-2$  eigenvectors which are of the form

$$\varphi_j = \text{col}[S(\delta_j, M-1), -1, S(0, P), \mathcal{L}_1 S(\delta_j, M-1), -\mathcal{L}_1, S(0, P)],$$

$$\varphi_{M+k} = \text{col}[S(0, M), S(\delta_k, P-1), -1, S(0, M), \mathcal{L}_1 S(\delta_k, P-1), \mathcal{L}_1],$$

with  $j = 1, 2, \dots, M-1, k = 1, 2, \dots, P-1$ . The symbol  $S(0, N)$  indicates a sequence of  $N$  zeros. These eigenvectors are associated with antiphased solutions in which only a pair of modes in one polarization is excited but with opposite phases. With these eigenvectors we construct the general solution of Eqs. (17)–(20):

$$x_{m1} = \alpha_m(\sigma) e^{iT} + \text{c.c.}, \quad y_{p1} = \beta_p(\sigma) e^{iT} + \text{c.c.}, \quad (28)$$

$$u_{m1} = \mathcal{L}_1 \alpha_m(\sigma) e^{iT} + \text{c.c.}, \quad v_{p1} = \mathcal{L}_1 \beta_p(\sigma) e^{iT} + \text{c.c.} \quad (29)$$

The coefficients of the solutions satisfy the separate sum rules

$$\sum_{m=1}^M \alpha_m(\sigma) = 0, \quad \sum_{p=1}^P \beta_p(\sigma) = 0. \quad (30)$$

The functions  $\alpha_m(\sigma)$  and  $\beta_p(\sigma)$  will be determined by requiring that solutions at order  $\delta^3$  be periodic.

$$\varphi = \text{col}[(1/M)S(1, M), (-1/P)S(1, P), (\mathcal{L}_2/M)S(1, M), (-\mathcal{L}_2/P)S(1, P)],$$

$$\mathcal{L}_2 = (\beta - 1)G_{h2}/(i\omega + \gamma_{h2}/G_{h2}).$$

The notation  $S(1, M)$  stands for  $M$  consecutive 1. This eigenvector is associated with solutions where all modes in each polarization are excited and have the same phase, but the two polarizations have opposite phases. With this eigenvector we can construct the general solutions of Eqs. (17)–(20) at  $I_h = I_{h2}$ :

$$x_{m1} = [\alpha(\sigma)/M] e^{iT} + \text{c.c.}, \quad (31)$$

$$y_{p1} = -[\alpha(\sigma)/P] e^{iT} + \text{c.c.},$$

$$u_{m1} = [\mathcal{L}_2 \alpha(\sigma)/M] e^{iT} + \text{c.c.}, \quad (32)$$

$$v_{p1} = -[\mathcal{L}_2 \alpha(\sigma)/P] e^{iT} + \text{c.c.}$$

This time, the coefficients of the solutions satisfy a global sum rule which couples the modes of the two polarizations:

$$\sum_{m=1}^M x_{m1}(\sigma) + \sum_{p=1}^P y_{p1}(\sigma) = 0. \quad (33)$$

The function  $\alpha(\sigma)$  will be determined by the solvability condition at the third order in the expansion in  $\delta$ .

(b)  $I_h = I_{h2}$ . The solutions of Eq. (27) are

$$\lambda_1 = \pm 1 + \frac{i}{\omega} \frac{2MP}{N} \frac{g \epsilon I_{h2}}{\eta} \left[ \frac{g_1}{g} - 1 \right] + O(\eta),$$

$$\lambda_2^2 = 1 + O(\eta),$$

$$\lambda_3 = \pm \left[ \frac{1 + (N-1)\beta}{1-\beta} \right]^{1/2} + \frac{2i}{\omega} \frac{g \epsilon I_{h2}}{\eta} \left[ M^2 + P^2 - MP + 2MP \frac{g_1}{g} \right] + O(\eta).$$

The third root does not contribute to the long time limit since  $\text{Re}(i\lambda_3) < 0$ . The real part of  $i\lambda_1$  is positive for  $g > \frac{1}{2}$  and negative for  $g < \frac{1}{2}$ . Thus we only consider the domain  $g < \frac{1}{2}$ . The eigenvalue  $\lambda_2$  is nondegenerate and has an eigenvector of the form

## B. Second-order problem

To simplify the study of the next order equations, we write the set of equations (17)–(20) in the more compact form

$$\partial z_1 / \partial T = \mathcal{M} z_1,$$

where  $z_1$  is a  $2N$ -dimensional column vector

$$z_n = \text{col}[S(x_n, M), S(y_n, P), S(u_n, M), S(v_n, P)]$$

and  $\mathcal{M}$  is a  $2N \times 2N$  constant matrix. With this notation, we can write the equations at order  $\delta^2$  as

$$\partial z_2 / \partial T = \mathcal{M} z_2 + N(z_1), \quad (34)$$

with the nonlinear vector

$$N(z_1) = \text{col}[S(X, M), S(Y, P), S(U, M), S(V, P)]$$

defined through

$$\begin{aligned}
 X_m &= \frac{x_{m1}}{I_h} \frac{\partial x_{m1}}{\partial T}, \quad Y_p = \frac{y_{p1}}{J_h} \frac{\partial y_{p1}}{\partial T}, \\
 U_m &= \frac{1}{\omega} \left\{ a_2 + \frac{u_{m1}}{G_h} \left[ \omega \frac{\partial u_{m1}}{\partial T} + \frac{\gamma_h}{G_h} u_{m1} \right] \right\}, \\
 V_p &= \frac{1}{\omega} \left\{ a_2 + \frac{v_{p1}}{H_h} \left[ \omega \frac{\partial v_{p1}}{\partial T} + \frac{\gamma_h}{H_h} v_{p1} \right] \right\}.
 \end{aligned}$$

The solution of the second-order equations (34) is

$$x_{m2} = A_m + (B_m e^{2iT} + \text{c.c.}) + \bar{x}_m, \tag{35}$$

$$y_{p2} = C_p + (D_p e^{2iT} + \text{c.c.}) + \bar{y}_p,$$

$$u_{m2} = E_m + (F_m e^{2iT} + \text{c.c.}) + \bar{u}_m, \tag{36}$$

$$v_{p2} = G_p + (H_p e^{2iT} + \text{c.c.}) + \bar{v}_p,$$

where

$$\bar{z} = \text{col}[S(\bar{x}, M), S(\bar{y}, P), S(\bar{u}, M), S(\bar{v}, P)]$$

is the general solution of the homogeneous problem  $\partial \bar{z} / \partial T = \mathcal{M} \bar{z}$  which will not contribute to the leading approximation. The coefficients appearing in (35) and (36) are given in Appendix A.

**C. The third-order problem**

The third-order equations can be written as

$$\partial z_3 / \partial T = \mathcal{M} z_3 + N(z_1, z_2). \tag{37}$$

$$\psi_k(T) = \text{col}[S(\delta_k, M-1), -1, \mathcal{H}S(\delta_k, M-1), -\mathcal{H}]e^{iT},$$

$$\psi_{M+k}(T) = [\psi_k(T)]^*, \quad k = 1, 2, \dots, M-1, \quad \mathcal{H} = -\frac{I_{h1}}{\eta} \frac{1}{i\omega - \gamma_{h1}/G_{h1}}.$$

This gives  $2M - 2$  solutions. The remaining two solutions vanish in the long-time limit.

(ii)  $M, P \geq 1, N \geq 3$ , and  $I_h = I_{h1}$ . This domain requires  $g > \frac{1}{2}$  and the solutions of the homogeneous adjoint problem corresponding to the eigenvalue 1 are

$$\psi_k(T) = \text{col}[S(\delta_k, M-1), -1, S(0, P), \mathcal{H}S(\delta_k, M-1), -\mathcal{H}, S(0, P)]e^{iT}, \tag{40}$$

$$\psi_{M+l}(T) = \text{col}[S(0, M), S(\delta_l, P-1), -1, S(0, M), \mathcal{H}S(\delta_l, P-1), -\mathcal{H}]e^{iT}, \tag{41}$$

$$\psi_{N+k}(T) = [\psi_k(T)]^*, \quad \psi_{N+M+l}(T) = [\psi_{M+l}(T)]^*,$$

with  $k = 1, 2, \dots, M-1$  and  $l = 1, 2, \dots, P-1$ . This gives  $2N - 4$  solutions. The other four solutions vanish in the long-time limit.

(iii)  $M, P \geq 1, N \geq 3, I_h = I_{h2}$ , which requires  $g < \frac{1}{2}$ . There are only two solutions of the homogeneous problem which do not vanish in the long-time limit:

$$\psi_1(T) = \text{col}[(1/M)S(1, M), (-1/P)S(1, P), (\mathcal{H}/M)S(1, M), (-\mathcal{H}/P)S(1, P)]e^{iT}, \tag{42}$$

$$\psi_2(T) = [\psi_1(T)]^*.$$

**2. The amplitude equations**

With these expressions, it is not difficult to derive from the solvability conditions (38) the amplitude equations. These amplitude equations are fairly intricate. They are given explicitly in Appendix C. Here we shall simply give the structure of the equation which is sufficient to follow the discussion.

The nonlinear vector

$$N(z_1, z_2) = \text{col}[S(X, M), S(Y, P), S(U, M), S(V, P)]$$

has components which are defined in Appendix B. The homogeneous solutions of Eq. (37) has oscillations at the frequency 1. Since the inhomogeneous term  $N(z_1, z_2)$  has oscillations at the same frequency, bounded periodic solutions are possible if and only if the solvability conditions are satisfied [16]. There are  $2N$  solvability conditions

$$\int_0^{2\pi} \langle N(z_1, z_2) \cdot \psi_k(T) \rangle dT = 0, \quad k = 1, \dots, 2N, \tag{38}$$

where the scalar product of two vectors  $a = \text{col}[S(a, 2N)]$  and  $b = \text{col}[S(b, 2N)]$  is defined through  $\langle a \cdot b \rangle = \sum_k^{2N} a_k b_k^*$  and the asterisk means the complex conjugate. In the solvability condition (38) the  $\psi_k(T)$  are the solutions of the adjoint of the homogeneous problem  $\partial z / \partial T = \mathcal{M} z$  which we determine now.

**1. Solutions of the adjoint problem**

The solutions corresponding to the eigenvalue 1 are the following.

(i)  $M = N, P = 0$ , and  $I_h = I_{h1}$ .

(i)  $M = N, P = 0$ , and  $I_h = I_{h1}$ .

$$\begin{aligned}
 d\alpha_m(\sigma) / d\sigma &= \sum_q a_{mq} \alpha_q(\sigma) \\
 &+ \sum_{q,r,s} A_{mqs} \alpha_q(\sigma) \alpha_r(\sigma) \alpha_s^*(\sigma), \tag{43}
 \end{aligned}$$

with  $1 \leq m \leq M$ . These equations derive from the solva-

bility condition (38) using the solutions (39). Although we have written  $M$  equations for symmetry reasons, the sum rule (26) is automatically fulfilled, which means that there are only  $M-1$  independent equations in the set (43). The remaining  $M-1$  equations are simply the complex conjugates of Eq. (43).

(ii)  $M, P \geq 1, N \geq 3, I_h = I_{h1}$ , corresponding to the range  $g > \frac{1}{2}$ . Here, we neglect the difference between  $I_h$  and  $J_h$  and between  $G_h$  and  $H_h$  which are of order  $\epsilon$ . This leads to

$$\begin{aligned} d\alpha_m(\sigma)/d\sigma = & \sum_q b_{mq} \alpha_q(\sigma) \\ & + \sum_{q,r,s} \alpha_q(\sigma) [B_{mqs} \alpha_r(\sigma) \alpha_s^*(\sigma) \\ & \quad + C_{mqs} \beta_r(\sigma) \beta_s^*(\sigma)], \end{aligned} \quad (44)$$

$$\begin{aligned} d\beta_p(\sigma)/d\sigma = & \sum_q c_{mq} \beta_q(\sigma) \\ & + \sum_{q,r,s} \beta_q(\sigma) [D_{pqs} \beta_r(\sigma) \beta_s^*(\sigma) \\ & \quad + E_{pqs} \alpha_r(\sigma) \alpha_s^*(\sigma)], \end{aligned}$$

for  $1 \leq m \leq M$  and  $1 \leq p \leq P$ . These equations derive from the solvability condition (38) using the solutions (40) and (41). We have written  $N$  equations for symmetry reasons but since the sum rule (30) is automatically satisfied there are only  $N-2$  independent equations in the set (44). The other  $N-2$  equations are the complex conjugates of Eq. (44).

(iii)  $M, P \geq 1, N \geq 3, I_h = I_{h2}$ , corresponding to the range  $g < \frac{1}{2}$ .

$$\begin{aligned} d\alpha_m(\sigma)/d\sigma = & \sum_q d_{mq} \alpha_q(\sigma) + \sum_{q,r,s} F_{mqs} \alpha_q(\sigma) \alpha_r(\sigma) \alpha_s^*(\sigma). \end{aligned} \quad (45)$$

This equation derives from the solvability condition (38) using the solution (42).

### III. CLASSIFICATION AND STABILITY CONDITIONS FOR PERIODIC SOLUTIONS

To solve Eqs. (43)–(45) still represents a formidable task. Instead, we shall consider the four classes of solutions which have been identified in [5] and we shall study their stability using Eqs. (43)–(45). With this trade-off, we shall be able to determine the stability of the solutions which we know, but we shall not know whether other stable periodic solutions emerge from the Hopf bifurcations.

#### A. $M = N > 2, P = 0, I_h = I_{h1}$

For this case,  $\alpha_m(\sigma)$  must satisfy the sum rule (26). Two solutions which satisfy the above condition are as follows.

##### (a) AD1 solutions.

$$\alpha_m(\sigma) = \rho(\sigma) e^{2\pi i m \sigma / M}, \quad (46)$$

where  $r = 1, 2, \dots, M-1$  and  $m = 1, \dots, M$ . From Eq. (43), the complex amplitude  $\rho(\sigma)$  satisfies the equation

$$\begin{aligned} \frac{d\rho(\sigma)}{d\sigma} = & \frac{i\omega c_1}{I_h} \left[ \rho(\sigma) A_m + \rho^*(\sigma) B_m - \frac{1}{I_h} \rho^2(\sigma) \rho^*(\sigma) \right] \\ & + \frac{\mathcal{H}^* c_1}{G_h} \{ c_2 [\mathcal{L}_1 \rho(\sigma) E_m + \mathcal{L}_1^* \rho^*(\sigma) F_m] \\ & \quad - a_2 \mathcal{L}_1 \rho(\sigma) - c_3 \rho^2(\sigma) \rho^*(\sigma) \}. \end{aligned} \quad (47)$$

The coefficients  $A_m, B_m, E_m$ , and  $F_m$  are those given in Appendix A after replacing  $\alpha_m(\sigma)$  by  $\rho(\sigma)$ . In the AD1 regime, all modes have the same amplitude, each mode being phase shifted by  $1/M$  of the period from another mode.

For this discussion, the choice of  $m$  is irrelevant since the set  $\{\alpha_m(\sigma)\}$  is the same for any  $m$  in the range  $[1, M-1]$ : different  $m$  correspond to different orderings of the sequence  $\{\alpha_m(\sigma)\}$ . This means that the solution (46) has a high degree of degeneracy: there are  $(M-1)!$  equivalent antiphased states. We have proposed in [6] a simple procedure to switch between the  $(M-1)!$  equivalent antiphased states obtained by permuting the  $M$  modes of a given antiphased state in (46). The polar decomposition  $\rho(\sigma) = R(\sigma) \exp[i\theta(\sigma)]$  leads to an equation for the real amplitude  $R(\sigma)$ ,

$$\frac{dR}{d\sigma} = \xi_1 a_2 R + \xi_3 R^3 = [\xi_{10} + O(\eta)] a_2 R + [\xi_{30} + O(\eta)] R^3. \quad (48)$$

In all cases treated in this paper, the linear coefficient  $\xi_{10}$  does not vanish. This equation has two solutions. The trivial solution  $R=0$  corresponds to the steady-state solution. The nontrivial solution  $R^2 = -\xi_1 a_2 / \xi_3$  corresponds to the self-pulsing solution. Since  $R^2$  must be positive,  $a_2$  and  $\xi_1 / \xi_3$  must have the opposite sign. When  $a_2 < 0$  the bifurcation at  $I_h = I_{h1}$  is subcritical and the self-pulsing solution, AD1, is unstable. When  $a_2 > 0$  the bifurcation is supercritical and the self-pulsing solution is stable near  $I_{h1}$ . We can show analytically that  $\xi_{30} = 0$  which means that the bifurcation becomes vertical in the limit  $\eta \rightarrow 0$ . Figure 1(a) shows the dependence of  $\xi_1 / \xi_3$  on the geometrical factor  $g$  for the case of  $M=3$  and  $P=0$ . From the parameters of this figure, the AD1 regime is always stable. The corresponding bifurcation diagram is shown in Fig. 1(b) where it is clear that the bifurcation is indeed almost vertical for  $\eta \rightarrow 0$ .

(b) AD2 solutions. For the same values of the parameters as in the AD1 regime, we find another solution in which  $L$  of the  $M$  modes are in phase and the other  $J = M - L$  modes are also in phase, but the two subsets antiphase. We shall refer to this solution as AD2. From the sum rule (26) it follows that the amplitudes in the AD2 regime must be given by

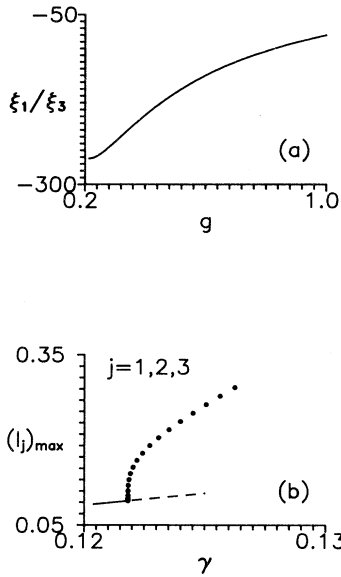


FIG. 1. The AD1 regime. (a) The dependence of  $\xi_1/\xi_3$  on the geometrical factor  $g$ . (b) Bifurcation diagram for  $g=0.52$ . Parameters are  $M=3$ ,  $P=0$ ,  $\alpha=0.1$ ,  $\beta=0.6$ ,  $\epsilon=5\times 10^{-3}$ ,  $\eta=2\times 10^{-4}$ , and  $I_h=I_{h1}$ . Full line: stable steady state; dashed line: unstable steady state; black dots: maxima of the stable periodic solution.

$$\alpha_m(\sigma)=\rho(\sigma)/L, \quad \alpha_n(\sigma)=-\rho(\sigma)/J, \\ m=1,2,\dots,L, \quad n=1,2,\dots,J. \quad (49)$$

In polar coordinates,  $\rho(\sigma)=R(\sigma)\exp[i\theta(\sigma)]$  and the modulus of  $\rho(\sigma)$  satisfies an equation which has the same structure as (48) except for the fact that in this regime  $\xi_{30}\neq 0$ , so we can neglect the corrections of order  $\eta$ . Figure 2(a) shows the dependence of  $\xi_{10}/\xi_{30}$  on the geometrical factor  $g$  for the case of  $M=3$  and  $P=0$ . The AD2 regime is stable for the parameters of Fig. 2(a). The corresponding bifurcation diagram is shown in Fig. 2(b). It is clear from this figure that the relation

$$[(I_3)_{\max}-I_h]/[(I_{1,2})_{\max}-I_h]=|\alpha_n/\alpha_m|=L/J$$

holds with  $L=2$  and  $J=1$ .

### B. $M$ and $P \geq 1$ , $N \geq 3$ , $I_h=I_{h1}$ ( $g > \frac{1}{2}$ )

For this case,  $\alpha_m(\sigma)$  and  $\beta_p(\sigma)$  must satisfy the separate sum rules (30) for each polarization. A solution which satisfies these conditions is

$$\alpha_m(\sigma)=\rho_1(\sigma)e^{2\pi imr/M}, \quad \beta_p(\sigma)=\rho_2(\sigma)e^{2\pi ipn/P}, \quad (50)$$

where the ranges of  $r$ ,  $m$ ,  $n$ , and  $p$  are from 1 to  $M-1$ ,  $M$ ,  $P-1$ , and  $P$  respectively. We call the solution (50) the AD3 regime. It is a regime in which all modes in each polarization are antiphased as in AD1. We have in this way a periodic solution in which all modal intensities in a given polarization have the same period and the same amplitude. The ratio of the periods  $M/P$  is given

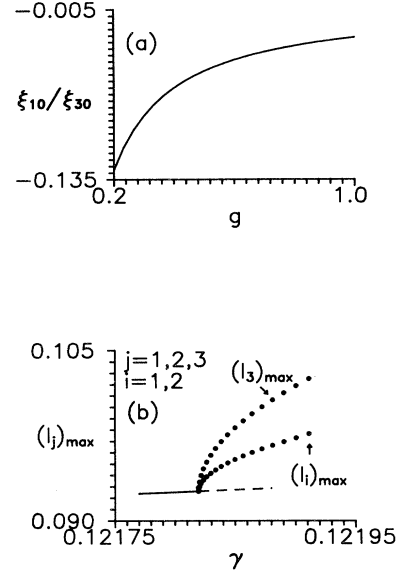


FIG. 2. The AD2 regime. (a) The dependence of  $\xi_{10}/\xi_{30}$  on the geometrical factor  $g$ . (b) Bifurcation diagram for  $g=0.52$ . Same parameters and conventions as in Fig. 1.

by the ratio of the mode number in the two polarizations. An exception, however, is the case  $P=1$  and  $M > 1$ , for which  $\beta_1(\sigma)=0$  and the amplitude of the corresponding mode is not determined at this order of the expansion in  $\eta$ . With the decomposition  $\rho_1(\sigma)=R_1(\sigma)\exp[i\theta_1(\sigma)]$  and  $\rho_2(\sigma)=R_2(\sigma)\exp[i\theta_2(\sigma)]$ , the moduli of  $\rho_1(\sigma)$  and  $\rho_2(\sigma)$  satisfy the equations

$$\frac{dR_1}{d\sigma}=R_1(\xi_1 a_2 + \xi_3 R_1^2 + \xi_2 R_2^2) \\ =[\xi_{10} + O(\eta)]a_2 R_1 + [\xi_{30} + O(\eta)]R_1^3 + \xi_2 R_1 R_2^2, \quad (51)$$

$$\frac{dR_2}{d\sigma}=R_2(\xi_1 a_2 + \xi_3 R_2^2 + \xi_2 R_1^2) \\ =[\xi_{10} + O(\eta)]a_2 R_2 + [\xi_{30} + O(\eta)]R_2^3 + \xi_2 R_2 R_1^2, \quad (52)$$

where  $\xi_1$ ,  $\xi_2$ , and  $\xi_3$  ( $\xi_1$ ,  $\xi_2$ , and  $\xi_3$ ) are functions of  $A_m$ ,  $B_m$ ,  $E_m$ , and  $F_m$  ( $C_p$ ,  $D_p$ ,  $G_p$ , and  $H_p$ ). Let us discuss the stability conditions for some special cases.

(a)  $M > 2$  and  $P=1$ . For this case,  $\zeta_2=\xi_2=0$ . Furthermore the sum rule on the  $P$  modes implies  $R_2=0$ . For the modes  $M > 2$ , we can prove analytically that  $\xi_{30}=0$ , which means that the bifurcation is vertical in the limit  $\eta \rightarrow 0$ .

(b)  $M$  and  $P > 2$ . The coefficients  $\zeta_2$  and  $\xi_2$  vanish. Both coefficients  $\xi_{30}$  and  $\zeta_{30}$  vanish in the limit  $\eta \rightarrow 0$ . For  $\eta \neq 0$ , we have not been able to draw any analytical conclusion.

(c)  $M=2$  and  $P=1$ . Here again  $\zeta_2=\xi_2=0$  and  $R_2=0$ . We can prove analytically that  $\xi_{30}\neq 0$ , so we can neglect the corrections of order  $\eta$ . Figure 3(a) shows the dependence of  $\xi_{10}/\xi_{30}$  on the geometrical factor  $g$  for this case.

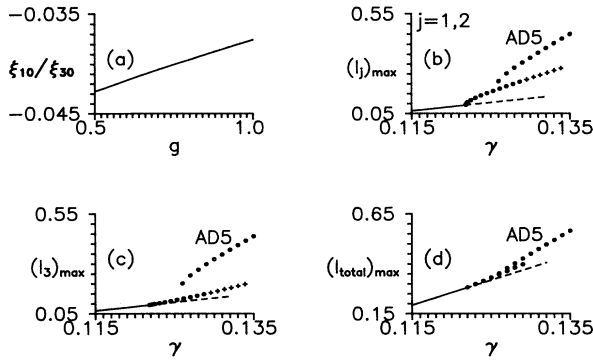


FIG. 3. The AD3 regime for  $M=2$  and  $P=1$ . The other parameters are as in Fig. 1. (a) The dependence of  $\xi_{10}/\xi_{30}$  on the geometrical factor  $g$ . (b)–(d) Bifurcation diagrams for the two  $M$  modes, for the  $P$  mode, and for the total intensity, respectively, with  $g=0.52$ . Same conventions as in Fig. 1. The plus signs are the maxima of the unstable periodic solutions.

The AD3 regime is stable for the parameters of this figure. The corresponding bifurcation diagram is shown in Figs. 3(b)–3(d).

For the remaining cases, either  $M > 2$ ,  $P=2$  with  $\xi_2=0$  and  $\xi_2 \neq 0$  or  $M=P=2$  with  $\xi_2 \neq 0$  and  $\xi_2 \neq 0$ . The main point is that in these cases the nonlinear coefficients have the property  $\xi_{30} \neq 0$  and  $\xi_{30} \neq 0$ .

### C. $M$ and $P \geq 1$ , $N \geq 3$ , $I_h = I_{h2}$ ( $g < \frac{1}{2}$ )

From the eigenvector corresponding to this case, the only possible solution is

$$\alpha_m(\sigma) = \rho(\sigma)/M, \quad \beta_p(\sigma) = -\rho(\sigma)/P. \quad (53)$$

This means that the two polarizations antiphase, while all the modes in each polarization are in phase. We refer to this regime as AD4. The modulus of  $\rho(\sigma)$  satisfies an equation of the form (51) with  $\xi_{30} \neq 0$ , so we can neglect the corrections of order  $\eta$ . Figure 4(a) shows the dependence of  $\xi_{10}/\xi_{30}$  on the geometrical factor  $g$  for the case of  $M=2$  and  $P=1$ . Thus the AD4 regime is stable for

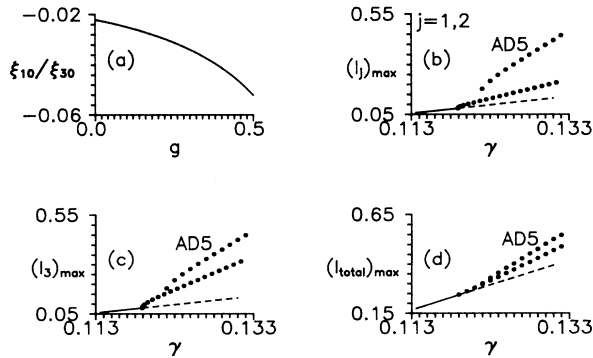


FIG. 4. The AD4 regime for  $M=2$  and  $P=1$ . (a) The dependence of  $\xi_{10}/\xi_{30}$  on the geometrical factor  $g$ . (b)–(d) Bifurcation diagrams for the two  $M$  modes, for the  $P$  mode, and for the total intensity, respectively, with  $g=0.48$ . Same parameters and conventions as in Fig. 1.

the parameters of Fig. 4(a). The corresponding bifurcation diagram is shown in Figs. 4(b)–4(d).

The reason for discussing how the coefficients depend on  $\eta$  is related to the scaling laws. In all the cases we have considered here, the linear coefficient was finite in the limit of vanishing  $\eta$ . If the coefficient of the nonlinear term also remains finite, the amplitudes of the periodic solutions satisfy the scaling  $R^2 \sim \mu - \mu_h$  where  $\mu$  is the control parameter and  $\mu_h$  is its value at the Hopf bifurcation. Typical choices for the control parameter are the linear gain or the cavity losses. In contrast, if the nonlinear coefficient in the amplitude equations vanishes in the limit  $\eta \rightarrow 0$ , the scaling law take the nongeneric form  $R^n \sim \mu - \mu_h$  where  $n = n(\eta)$ . A simpler form of nongeneric scaling occurs, for instance, when  $M \geq 2$  and  $P=1$ . In this case the  $M$  modes have a regular scaling while the isolated  $P$  mode scales like  $R^2 \sim (\mu - \mu_h)^2$  because  $R$  must vanish to dominant order. Examples of nongeneric scalings have been given in [5].

## IV. NUMERICAL RESULTS

We have studied analytically the periodic solutions emerging from the Hopf bifurcation and their stability near the bifurcation. Numerical simulations beyond the Hopf bifurcation have been carried out to characterize the solutions away from the bifurcation point.

The general feature we have observed is the emergence from the three regimes AD1, AD3, and AD4 of a new regime, which we call AD5. At the point where the AD5 regime appears, it is characterized by the same type of symmetry properties as the AD1 regime: all modes have the same periodic temporal dependence but are phase shifted from each other by  $1/N$  of the period if  $N$  modes oscillate. This remains true even if the modes are partitioned among the two directions of polarization. However, the sum rule (26) is no longer satisfied: the sum of the intensities deviates markedly from the steady-state sum. Another feature of the AD5 regime is that upon increasing the pump parameter it evolves from a simple periodic state (period-1 solution) towards chaos via a sequence of bifurcations, either the classic Feigenbaum sequence or variants of it where some of the subharmonic bifurcations are missing. For the three cases analyzed in Fig. 5, where

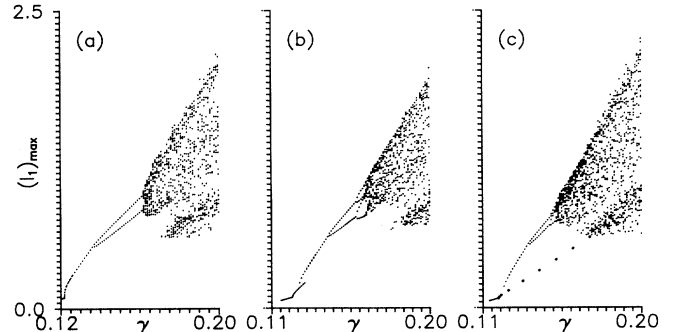


FIG. 5. Bifurcation diagrams for the first mode. (a) Parameters are as in Fig. 1. (b) Parameters are as in Fig. 3. (c) Parameters are as in Fig. 4.

$N = 3$ , we noticed that throughout the transition from the period-1 state to the first chaotic domain the modes remain antiphased: the total intensity has a peak in its power spectrum at three times the fundamental frequency of the individual modes. In other chaotic domains which occur for still larger values of the control parameter, the power spectrum of the total intensity may display a peak at twice the dominant frequency of the individual modes, but we have not observed any case where the total intensity has a peak at such low frequency as the individual modes.

In Fig. 1(b), the solutions AD1 change smoothly into the new regime AD5. In this case it is difficult to determine a point at which the transition occurs. In Fig. 5(a) we display the maxima of the periodic solution over a larger domain of the pump parameter  $\gamma$ . The points on a given vertical are the maxima of  $I_1$ . A large domain of chaos appears which is connected to the period-1 solution via a nonstandard sequence of bifurcations.

In Fig. 2(b), we display the AD2 regime which remains stable but the sum rule (26) is no longer satisfied: the average of the total intensity increases and is time periodic. However, no instability of this branch has been observed.

In Figs. 3(b)–3(d), we observe that the branch of solutions which emerges from the bifurcation point becomes unstable at a finite distance of the first bifurcation. At that secondary bifurcation, the solution jumps to another branch which is an AD5 regime. There is an overlap between the stable domains of these two branches. For larger values of the pump parameter, a classic Feigenbaum sequence leads to chaos. It is shown in Fig. 5(b).

In Figs. 4(b)–4(d), the branch of AD4 solutions remains stable and no instability point has been observed. The only change is again a departure from the sum rule (33): the total intensity deviates from its steady-state value and becomes time periodic. However, when a sufficiently large perturbation is applied to the system, a new branch of stable periodic states is revealed. It is again an AD5 regime and we show in Fig. 5(c) that this new branch bifurcates to chaos. In this case the AD4 regime remains stable over the whole domain we have investigated.

For the AD3 regime, we have shown that the Hopf bifurcation can be regular or nearly vertical, depending on the number of modes. To be complete, we display in Fig. 6 bifurcation diagrams for  $M = 3$  and  $P = 1$ . The three modes  $M$  undergo a nearly vertical bifurcation while the mode  $P$  has very small amplitude oscillations over a long domain of the control parameter. Figure 6(a) shows the maxima of the solutions near the Hopf bifurcation. In Fig. 6(b), we display the bifurcation diagram for one of the  $M$  modes. The AD3 branch which emerges from the Hopf bifurcation suddenly changes into a breather mode: the envelope of the AD3 solution is modulated at a very low frequency and with a small amplitude. This breather mode becomes unstable and the solution jumps to the AD5 branch. The AD5 branch is associated with a simple periodic solution for low  $\gamma$ . For larger  $\gamma$ , a breather mode appears again, which is then followed by a complex sequence of periodic and chaotic states. For the two

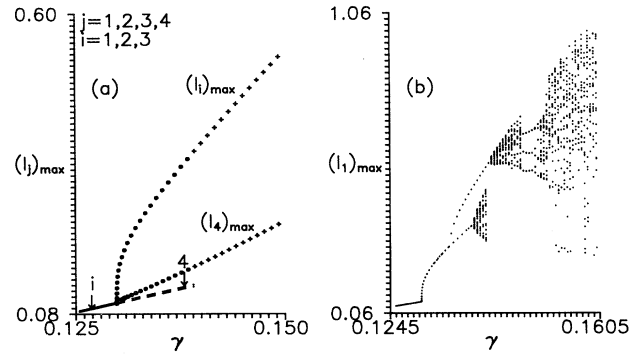


FIG. 6. The AD3 regime for  $M = 3$  and  $P = 1$ . The other parameters are as in Fig. 3. (a) Bifurcation diagram near the Hopf bifurcation. (b) Bifurcation diagram for larger values of the pump parameter.

branches of solutions displayed in Fig. 6(b), the quasi-periodic regimes preserve the antiphase dynamics: the envelope modulation of the modal intensities are shifted by  $1/N$  of the period.

## V. CONCLUSION

We have shown in this paper that the periodic solutions which emerge from a Hopf bifurcation in ISHG can be studied analytically in the vicinity of the bifurcation point. Using the deviation of the pump parameter from its value at the Hopf bifurcation as a small parameter, we have made a systematic expansion around the bifurcation point and derived in the usual way bifurcation equations which rule the time evolution of the amplitude of the periodic solutions. Since there are  $N$  complex nonlinear amplitude equations associated with  $N$  modes, there is no hope for a general discussion of the properties of these equations. Therefore we have analyzed only those solutions which had been found numerically in previous studies. We have shown that a useful way to characterize these solutions is via sum rules which apply either to each polarization or to the global system. One merit of the approach followed in this paper is to clarify some basic problems related to the nature of the Hopf bifurcation. In particular, the qualitative discussion in Sec. III indicates the ISHG is prone to generate vertical Hopf bifurcations at  $I_{h1}$ . It also indicates that for a given type of AD the Hopf bifurcation can change from supercritical to vertical as a function of the number of modes which oscillate. Finally, our numerical simulation has indicated that, as the pump parameter is increased, the general trend in ISHG is the transition to a new regime which we called AD5. It is characterized by a global behavior in the sense that the division into orthogonal polarizations is no longer relevant. It is also the simplest of the four regimes identified so far near the Hopf bifurcation points. Finally, the AD5 regime has the expected complex behavior with routes to chaos and chaotic regimes which retain some of the mode correlations characteristic of AD.

## ACKNOWLEDGMENTS

Fruitful discussions with T. Erneux are gratefully acknowledged. This research was supported in part by the Fonds National de la Recherche Scientifique (Belgium) and by the Interuniversity Attraction Pole program of the Belgian government.

## APPENDIX A: COEFFICIENTS OF THE SECOND-ORDER SOLUTION

The coefficients appearing in the second-order solution (35) and (36) are as follows.

1. AD1 ( $M = N, P = 0$ , and  $I_h = I_{h1}$ )

$$A_m = \frac{a_2 + 2g\epsilon(1-\beta)\alpha_m(\sigma)\alpha_m^*(\sigma) - [\beta G_h + 2g\epsilon\gamma_h/G_h]Y_a}{(1-\beta)G_h - g\epsilon\gamma_h/G_h},$$

$$E_m = -g\epsilon \frac{a_2 + 2g\epsilon(1-\beta)\alpha_m(\sigma)\alpha_m^*(\sigma) - (2-\beta)G_h Y_a}{(1-\beta)G_h - g\epsilon\gamma_h/G_h},$$

$$B_m = \frac{2}{3I_h}\alpha_m^2(\sigma) - \frac{i\omega\eta}{3\omega_h} \left[ \frac{\gamma_h}{I_h G_h} - (1-\beta) \right] \alpha_m^2(\sigma) - \frac{(1-\beta)\eta\gamma_h}{3\omega_h G_h} \alpha_m^2(\sigma),$$

$$F_m = \frac{\eta}{I_h} \left[ 2i\omega - \frac{\gamma_h}{G_h} \right] B_m - \frac{i\omega\eta}{I_h^2} \alpha_m^2(\sigma),$$

where

$$\omega_h = (1-\beta)I_h G_h - \eta \left[ \frac{\gamma_h}{G_h} \right]^2,$$

$$Y_a = \frac{Ma_2 + 2g\epsilon(1-\beta) \sum_{j=1}^M \alpha_j(\sigma)\alpha_j^*(\sigma)}{[1+(M-1)\beta]G_h + (2M-1)g\epsilon}.$$

2. AD2 ( $M = N = L + J, P = 0$ , and  $I_h = I_{h1}$ )

$$A_m = \frac{a_2}{[1+(M-1)\beta]G_h} + O(\eta),$$

$$A_n = \frac{a_2}{[1+(M-1)\beta]G_h} + O(\eta),$$

$$E_m = O(\eta), \quad E_n = O(\eta),$$

$$B_m = B_{m0} + i\omega\eta B_{m1} + O(\eta), \quad B_n = B_{n0} + i\omega\eta B_{n1} + O(\eta),$$

$$F_m = i\omega\eta F_{m1} + O(\eta), \quad F_n = i\omega\eta F_{n1} + O(\eta),$$

where  $n = 1, 2, \dots, J, m = 1, 2, \dots, L$ , and

$$B_{m0} = \frac{2}{3I_h}\alpha_m^2(\sigma) - \frac{2}{3I_h} \frac{\beta}{M\beta - 3(1-\beta)} \left[ \sum_{r=1}^L \alpha_r^2(\sigma) + \sum_{k=1}^J \alpha_k^2(\sigma) \right],$$

$$B_{n0} = \frac{2}{3I_h}\alpha_n^2(\sigma) - \frac{2}{3I_h} \frac{\beta}{M\beta - 3(1-\beta)} \left[ \sum_{r=1}^L \alpha_r^2(\sigma) + \sum_{k=1}^J \alpha_k^2(\sigma) \right],$$

$$F_{m1} = \frac{1}{3I_h^2}\alpha_m^2(\sigma) - \frac{4}{3I_h^2} \frac{\beta}{M\beta - 3(1-\beta)} \left[ \sum_{r=1}^L \alpha_r^2(\sigma) + \sum_{k=1}^J \alpha_k^2(\sigma) \right],$$

$$F_{n1} = \frac{1}{3I_h^2}\alpha_n^2(\sigma) - \frac{4}{3I_h^2} \frac{\beta}{M\beta - 3(1-\beta)} \left[ \sum_{r=1}^L \alpha_r^2(\sigma) + \sum_{k=1}^J \alpha_k^2(\sigma) \right],$$

$$B_{m1} = \frac{1}{3I_h G_h} \alpha_m^2(\sigma) - \frac{2g(\epsilon/\eta)}{3(1-\beta)G_h} B_{m0} + \frac{4g(\epsilon/\eta)}{3(1-\beta)G_h} \left[ \sum_{r=1}^L B_{r0} + \sum_{k=1}^J B_{k0} \right] + \frac{1}{3(1-\beta)G_g} \frac{\gamma_h}{G_h} F_{m1} + \frac{\beta}{3(1-\beta)} Y_b,$$

$$B_{n1} = \frac{1}{3I_h G_h} \alpha_n^2(\sigma) - \frac{2g(\epsilon/\eta)}{3(1-\beta)G_h} B_{n0} + \frac{4g(\epsilon/\eta)}{3(1-\beta)G_h} \left[ \sum_{r=1}^L B_{r0} + \sum_{k=1}^J B_{k0} \right] + \frac{1}{3(1-\beta)G_h} \frac{\gamma_h}{G_h} F_{n1} + \frac{\beta}{3(1-\beta)} Y_b,$$

$$Y_b = -\frac{1-\beta}{[M\beta - 3(1-\beta)]I_h G_h} \left[ \sum_{r=1}^L \alpha_r^2(\sigma) + \sum_{k=1}^J \alpha_k^2(\sigma) \right] - \frac{1}{[M\beta - 3(1-\beta)]G_h} \frac{\gamma_h}{G_h} \left[ \sum_{r=1}^L F_{r1} + \sum_{k=1}^J F_{k1} \right] + \frac{2(1-2M)g(\epsilon/\eta)}{[M\beta - 3(1-\beta)]G_h} \left[ \sum_{r=1}^L B_{r0} + \sum_{k=1}^J B_{k0} \right].$$

3.  $M, P \geq 1, I_h = I_{h1}$  or  $I_{h2}$ 

$$A_m = \frac{a_2}{[1+(N-1)\beta]G_h} + O(\eta),$$

$$C_p = \frac{a_2}{[1+(N-1)\beta]G_h} + O(\eta),$$

$$E_m = O(\eta), \quad G_p = O(\eta),$$

$$B_m = B_{m0} + i\omega\eta B_{m1} + O(\eta), \quad D_p = D_{p0} + i\omega\eta D_{p1} + O(\eta),$$

$$F_m = i\omega\eta F_{m1} + O(\eta), \quad H_p = i\omega\eta H_{p1} + O(\eta),$$

where

$$\begin{aligned}
B_{m0} &= \frac{2}{3I_h} \alpha_m^2(\sigma) - \frac{2}{3I_h} \frac{\beta}{N\beta - 3(1-\beta)} \left[ \sum_{r=1}^M \alpha_r^2(\sigma) + \sum_{r=1}^P \beta_r^2(\sigma) \right], \\
D_{p0} &= \frac{2}{3I_h} \beta_p^2(\sigma) - \frac{2}{3I_h} \frac{\beta}{N\beta - 3(1-\beta)} \left[ \sum_{r=1}^M \alpha_r^2(\sigma) + \sum_{r=1}^P \beta_r^2(\sigma) \right], \\
F_{m1} &= \frac{1}{3I_h^2} \alpha_m^2(\sigma) - \frac{4}{3I_h^2} \frac{\beta}{N\beta - 3(1-\beta)} \left[ \sum_{r=1}^M \alpha_r^2(\sigma) + \sum_{r=1}^P \beta_r^2(\sigma) \right], \\
H_{p1} &= \frac{1}{3I_h^2} \beta_p^2(\sigma) - \frac{4}{3I_h^2} \frac{\beta}{N\beta - 3(1-\beta)} \left[ \sum_{r=1}^M \alpha_r^2(\sigma) + \sum_{r=1}^P \beta_r^2(\sigma) \right], \\
B_{m1} &= \frac{1}{3I_h G_h} \alpha_m^2(\sigma) - \frac{2g(\epsilon/\eta)}{3(1-\beta)G_h} B_{m0} + \frac{4g(\epsilon/\eta)}{3(1-\beta)G_h} \sum_{r=1}^M B_{r0} \\
&\quad + \frac{4g_1(\epsilon/\eta)}{3(1-\beta)G_h} \sum_{r=1}^P D_{r0} + \frac{1}{3(1-\beta)G_h} \frac{\gamma_h}{G_h} F_{m1} + \frac{\beta}{3(1-\beta)} Y_{bd}, \\
D_{p1} &= \frac{1}{3I_h G_h} \beta_p^2(\sigma) - \frac{2g(\epsilon/\eta)}{3(1-\beta)G_h} D_{p0} + \frac{4g(\epsilon/\eta)}{3(1-\beta)G_h} \sum_{r=1}^P D_{r0} \\
&\quad + \frac{4g_1(\epsilon/\eta)}{3(1-\beta)G_h} \sum_{r=1}^M B_{r0} + \frac{1}{3(1-\beta)G_h} \frac{\gamma_h}{G_h} H_{p1} + \frac{\beta}{3(1-\beta)} Y_{bd}, \\
Y_{bd} &= -\frac{1-\beta}{[N\beta - 3(1-\beta)]I_h G_h} \left[ \sum_{r=1}^M \alpha_r^2(\sigma) + \sum_{r=1}^P \beta_r^2(\sigma) \right] - \frac{1}{[N\beta - 3(1-\beta)]G_h} \frac{\gamma_h}{G_h} \left[ \sum_{r=1}^P F_{r1} + \sum_{r=1}^M H_{r1} \right] \\
&\quad + \frac{2g(\epsilon/\eta)}{[N\beta - 3(1-\beta)]G_h} \left\{ \left[ 1 - 2M - 2P \frac{g_1}{g} \right] \sum_{r=1}^M B_{r0} + \left[ 1 - 2P - 2M \frac{g_1}{g} \right] \sum_{r=1}^P D_{r0} \right\}.
\end{aligned}$$

#### APPENDIX B: THE NONLINEAR CONTRIBUTIONS TO THE THIRD-ORDER EQUATION

The inhomogeneous part of Eq. (37) is given by

$$\begin{aligned}
X_m &= \frac{x_{m1}}{I_h} \left[ \frac{\partial x_{m2}}{\partial T} - \frac{x_{m1}}{I_h} \frac{\partial x_{m1}}{\partial T} \right] + \frac{x_{m2}}{I_h} \frac{\partial x_{m1}}{\partial T} \\
&\quad - \frac{1}{\omega \eta} \frac{\partial x_{m1}}{\partial \sigma}, \\
Y_p &= \frac{y_{p1}}{J_h} \left[ \frac{\partial y_{p2}}{\partial T} - \frac{y_{p1}}{J_h} \frac{\partial y_{p1}}{\partial T} \right] + \frac{y_{p2}}{J_h} \frac{\partial y_{p1}}{\partial T} - \frac{1}{\omega \eta} \frac{\partial y_{p1}}{\partial \sigma}, \\
U_m &= \frac{u_{m1}}{\omega G_h} \left\{ \omega \frac{\partial u_{m2}}{\partial T} - a_2 + \frac{\gamma_h}{G_h} u_{m2} \right. \\
&\quad \left. - \frac{u_{m1}}{G_h} \left[ \omega \frac{\partial u_{m1}}{\partial T} + \frac{\gamma_h}{G_h} u_{m1} \right] \right\}
\end{aligned}$$

$$+ \frac{u_{m2}}{\omega G_h} \left[ \omega \frac{\partial u_{m1}}{\partial T} + \frac{\gamma_h}{G_h} u_{m1} \right] - \frac{1}{\omega} \frac{\partial u_{m1}}{\partial \sigma},$$

$$\begin{aligned}
V_p &= \frac{v_{p1}}{\omega H_h} \left\{ \omega \frac{\partial v_{p2}}{\partial T} - a_2 + \frac{\gamma_h}{H_h} v_{p2} \right. \\
&\quad \left. - \frac{v_{p1}}{H_h} \left[ \omega \frac{\partial v_{p1}}{\partial T} + \frac{\gamma_h}{H_h} v_{p1} \right] \right\} \\
&\quad + \frac{v_{p2}}{\omega H_h} \left[ \omega \frac{\partial v_{p1}}{\partial T} + \frac{\gamma_h}{H_h} v_{p1} \right] - \frac{1}{\omega} \frac{\partial v_{p1}}{\partial \sigma}.
\end{aligned}$$

#### APPENDIX C: THE AMPLITUDE EQUATIONS

In this Appendix, we give the explicit form of the solvability conditions. Eq. (43) which rules the AD1 regime is:

$$\begin{aligned}
\frac{d\alpha_m(\sigma)}{d\sigma} &= \frac{i\omega c_1}{I_h} \left[ \alpha_m(\sigma) A_m + \alpha_m^*(\sigma) B_m - \frac{1}{I_h} \alpha_m^2(\sigma) \alpha_m^*(\sigma) \right] \\
&\quad - \frac{i\omega c_1}{I_h} \frac{c_1}{M} \left[ \sum_{r=1}^M \alpha_r(\sigma) A_r + \sum_{r=1}^M \alpha_r^*(\sigma) B_r - \frac{1}{I_h} \sum_{r=1}^M \alpha_r^2(\sigma) \alpha_r^*(\sigma) \right] \\
&\quad + \frac{\mathcal{H}^* c_1}{G_h} \{ c_2 [\mathcal{L}_1 \alpha_m(\sigma) E_m + \mathcal{L}_1^* \alpha_m^*(\sigma) F_m] - a_2 \mathcal{L}_1 \alpha_m(\sigma) - c_3 \alpha_m^2(\sigma) \alpha_m^*(\sigma) \} \\
&\quad - \frac{\mathcal{H}^* c_1}{G_h} \frac{c_1}{M} \left\{ c_2 \left[ \mathcal{L}_1 \sum_{r=1}^M \alpha_r(\sigma) E_r + \mathcal{L}_1^* \sum_{r=1}^M \alpha_r^*(\sigma) F_r \right] - c_3 \sum_{r=1}^M \alpha_r^2(\sigma) \alpha_r^*(\sigma) \right\}, \tag{C1}
\end{aligned}$$

where

$$c_1 = \frac{1}{1 + \mathcal{L}_1 \mathcal{H}^*}, \quad c_2 = i\omega + \frac{2\gamma_h}{G_h}, \quad c_3 = \frac{1}{G_h} \left[ i\omega + \frac{3\gamma_h}{G_h} \right] \mathcal{L}_1^2 \mathcal{L}_1^* . \quad (\text{C2})$$

Equations (44) which rule the AD3 dynamics are

$$\begin{aligned} \frac{d\alpha_m(\sigma)}{d\sigma} = & \frac{i\omega c_1}{I_h} \left[ \alpha_m(\sigma) A_m + \alpha_m^*(\sigma) B_m - \frac{1}{I_h} \alpha_m^2(\sigma) \alpha_m^*(\sigma) \right] \\ & - \frac{i\omega}{I_h} \frac{c_1}{M} \left[ \sum_{r=1}^M \alpha_r(\sigma) A_r + \sum_{r=1}^M \alpha_r^*(\sigma) B_r - \frac{1}{I_h} \sum_{r=1}^M \alpha_r^2(\sigma) \alpha_r^*(\sigma) \right] \\ & + \frac{\mathcal{H}^* c_1}{G_h} \{ c_2 [\mathcal{L}_1 \alpha_m(\sigma) E_m + \mathcal{L}_1^* \alpha_m^*(\sigma) F_m] - a_2 \mathcal{L}_1 \alpha_m(\sigma) - c_3 \alpha_m^2(\sigma) \alpha_m^*(\sigma) \} \\ & - \frac{\mathcal{H}^* c_1}{G_h} \frac{c_1}{M} \left\{ c_2 \left[ \mathcal{L}_1 \sum_{r=1}^M \alpha_r(\sigma) E_r + \mathcal{L}_1^* \sum_{r=1}^M \alpha_r^*(\sigma) F_r \right] - c_3 \sum_{r=1}^M \alpha_r^2(\sigma) \alpha_r^*(\sigma) \right\} , \end{aligned} \quad (\text{C3})$$

$$\begin{aligned} \frac{d\beta_p(\sigma)}{d\sigma} = & \frac{i\omega c_1}{I_h} \left[ \beta_p(\sigma) C_p + \beta_p^*(\sigma) D_p - \frac{1}{I_h} \beta_p^2(\sigma) \beta_p^*(\sigma) \right] \\ & - \frac{i\omega}{I_h} \frac{c_1}{P} \left[ \sum_{r=1}^P \beta_r(\sigma) C_r + \sum_{r=1}^P \beta_r^*(\sigma) D_r - \frac{1}{I_h} \sum_{r=1}^P \beta_r^2(\sigma) \beta_r^*(\sigma) \right] \\ & + \frac{\mathcal{H}^* c_1}{G_h} \{ c_2 [\mathcal{L}_1 \beta_p(\sigma) G_p + \mathcal{L}_1^* \beta_p^*(\sigma) H_p] - a_2 \mathcal{L}_1 \beta_p(\sigma) - c_3 \beta_p^2(\sigma) \beta_p^*(\sigma) \} \\ & - \frac{\mathcal{H}^* c_1}{G_h} \frac{c_1}{M} \left\{ c_2 \left[ \mathcal{L}_1 \sum_{r=1}^P \beta_r(\sigma) G_r + \mathcal{L}_1^* \sum_{r=1}^P \beta_r^*(\sigma) H_r \right] - c_3 \sum_{r=1}^P \beta_r^2(\sigma) \beta_r^*(\sigma) \right\} , \end{aligned} \quad (\text{C4})$$

for  $1 \leq m \leq M$  and  $1 \leq p \leq P$ . Finally, Eq. (45) which rules the AD4 regime is given by

$$\begin{aligned} \frac{d\alpha(\sigma)}{d\sigma} = & \frac{i\omega c_1}{I_h} \frac{M+P}{MP} \left\{ \frac{A_m}{M} \alpha(\sigma) + \frac{C_p}{P} \alpha(\sigma) + \frac{B_m}{M} \alpha^*(\sigma) + \frac{D_p}{P} \alpha^*(\sigma) - \frac{1}{I_h} \left[ \frac{1}{M^3} + \frac{1}{P^3} \right] \alpha^2(\sigma) \alpha^*(\sigma) \right\} \\ & + \frac{\mathcal{H}^* c_1}{G_h} \frac{M+P}{MP} \left\{ c_2 \left[ \frac{\mathcal{L}_2 E_m}{M} \alpha(\sigma) + \frac{\mathcal{L}_2^* F_m}{M} \alpha^*(\sigma) + \frac{\mathcal{L}_2 G_p}{P} \alpha(\sigma) + \frac{\mathcal{L}_2^* H_p}{P} \alpha^*(\sigma) \right] \right. \\ & \left. - a_2 \mathcal{L}_2 \frac{M+P}{MP} \alpha(\sigma) - c_4 \left[ \frac{1}{M^3} + \frac{1}{P^3} \right] \alpha^2(\sigma) \alpha^*(\sigma) \right\} , \end{aligned} \quad (\text{C5})$$

where

$$c_4 = \frac{1}{G_h} \left[ i\omega + \frac{3\gamma_h}{G_h} \right] \mathcal{L}_2^2 \mathcal{L}_2^* . \quad (\text{C6})$$

- 
- [1] K. Wiesenfeld, C. Bracikowski, G. James, and R. Roy, *Phys. Rev. Lett.* **65**, 1749 (1990).  
[2] C. Bracikowski and R. Roy, *Chaos* **1**, 49 (1991); *Phys. Rev. A* **43**, 6455 (1991).  
[3] P. Mandel and J.-Y. Wang, *Opt. Lett.* **19**, 533 (1994).  
[4] J.-Y. Wang and P. Mandel, *Phys. Rev. A* **48**, 671 (1993).  
[5] J.-Y. Wang, P. Mandel, and T. Erneux, *Quantum Semiclass. Opt.* **7**, 169 (1995).  
[6] K. Otsuka, J.-Y. Wang, P. Mandel, and T. Erneux, *Quantum Semiclass. Opt.* (to be published).  
[7] E. A. Viktorov, D. R. Klemer, and M. A. Karim, *Opt. Commun.* **113**, 441 (1995).  
[8] K. Otsuka, *Phys. Rev. Lett.* **67**, 1090 (1991).  
[9] K. Otsuka, P. Mandel, M. Georgiou, and C. Etrich, *Jpn. J. Appl. Phys.* **32**, L318 (1993).  
[10] N. B. Abraham, L. L. Everett, C. Iwata, and M. B. Janicki, *SPIE Proc.* **2095**, 16 (1994).  
[11] K. Otsuka, D. Pieroux, and P. Mandel, *Opt. Commun.* **108**, 265 (1994).  
[12] D. Pieroux, P. Mandel, and K. Otsuka, *Opt. Commun.* **108**, 273 (1994).  
[13] C. L. Tang, H. Statz, and G. deMars, *J. Appl. Phys.* **34**,

- 2289 (1963).
- [14] P. Mandel, in *Quantum Optics VI*, edited by J. D. Harvey and D. F. Walls (Springer-Verlag, Heidelberg, 1994), p. 275.
- [15] R. Roy, C. Bracikowski, and G. James, in *Recent Developments in Quantum Optics*, edited by R. Inguva (Plenum, New York, 1994), p. 309.
- [16] G. Iooss and D. D. Joseph, *Elementary Stability and Bifurcation Theory* (Springer-Verlag, Heidelberg, 1980).